



Fermilab

\bar{p} Note #357

Energy Deposition in the \bar{p} Target Hall
Proton Beam Dump

W. S. Freeman
January, 1984

Energy Deposition in the \bar{p} Target Hall Proton Beam Dump

This note summarizes the results of a series of CASIM¹ calculations dealing with the design of the proton beam dump in the \bar{p} target hall. The spatial dependence of the energy deposition was calculated for several dump configurations to assess the cooling requirements for the dump, as well as to study the question of local heating and possible melting of the dump core. Cylindrical dump geometries compatible with the design of the Tevatron I target station² were assumed, consisting of a graphite core, sometimes followed by aluminum, and enclosed in an aluminum annulus. The dump was assumed to be recessed in thick iron shielding. Conceptually this design is similar to that of the Energy Doubler dump.³ Both target in and target out calculations were done for various configurations in which the radius and length of the graphite and aluminum components were varied. A 150 GeV/c incident proton beam was assumed with a Gaussian beam spot having $\sigma_x = \sigma_y = 0.04$ cm.

I. Overall Energy Deposition

Initial calculations assumed that the dump core was composed entirely of graphite, with a length of 170 cm and a radius of 7.62 cm. It was encased in a cylindrical aluminum box of wall thickness 1.27 cm. Fig. 1 shows the resulting deposited energy per incident proton per bin (left hand scale) versus the distance downstream from the target position, for the

four innermost radial bins. The bin dimensions were $\Delta Z=22$ cm and $\Delta r=7.62$ cm. Note that each curve represents the energy density per incident proton (the quantity calculated by CASIM) multiplied by the volume of the relevant bin. The solid dots in Fig. 1 are for the innermost radial bin and, because of the radial bin size chosen, represent the energy deposition in the graphite core. The right-hand scale represents the average power deposited assuming 3×10^{12} protons and a 2 sec cycle time. The sharp jump in deposited energy near $Z=550$ cm is due to the transition from graphite to iron at the end of the dump.

From the point of view of cooling requirements, a more uniform distribution of deposited energy is desirable. To reduce the sharp jump at the graphite-iron interface, a series of calculations was done in which varying lengths of aluminum replaced a portion of the graphite core. Fig. 2 shows the results when the last 50 cm of graphite was replaced by 50 cm of aluminum. The peak energy deposited in the iron was reduced by $\sim 14\%$, but a sharp transition still remained, with the maximum still in the iron. By extending the length of the aluminum part of the core to 100 cm (i.e., 120 cm of graphite followed by 100 cm of aluminum) the results shown in Fig. 3 were obtained. The sharp peak in the iron was reduced significantly, so that the maximum energy deposition occurred in the aluminum part of the core and is only $\sim 50\%$ of the maximum in Fig. 1.

Next, the radial dependence of the energy deposition was studied by varying the thickness of aluminum surrounding the 120 cm carbon + 100 cm aluminum core. Fig. 4 shows the results for a 7.62 cm aluminum annulus

surrounding the 7.62 cm radius core. The solid dots are the results for the core. The open circles represent the energy deposited in the annulus, while the solid triangles are for the third radial bin outward. This third bin is now the innermost bin of the iron shielding surrounding the dump. The effect of adding the aluminum annulus was to radially spread out the energy deposition, thus decreasing the deposited energy in the second radial bin and increasing it in the third bin, so that comparable amounts of energy were deposited in both bins.

To minimize the overall length of the dump, the calculation was repeated with the length of aluminum in the core reduced to 75 cm from 100 cm. The 7.62 cm aluminum annulus was retained. Fig. 5 displays the results. As expected, higher energy deposition occurred after the aluminum-iron interface in the dump core, but it is not much larger than the peak values that occur in the aluminum part of the core itself.

Based on the calculations outlined in this section, it appears that of the order of 100 cm of aluminum should follow a 120 cm long graphite core, while the addition of an aluminum annulus of 7.62 cm thickness surrounding this core makes the energy deposition more uniform in the radial direction. For this "optimum" geometry (see Fig. 7), the actual energy densities per proton are plotted in Fig. 6.

II. Heating of the Dump Core Within the Beam Region

CASIM¹ calculations with radial bin sizes comparable to the beam spot standard deviation, σ , were done to estimate heating within the beam region in the dump core. The particular dump geometry used was a graphite core of 7.62 cm radius and 120 cm length, followed by a 7.62 cm radius and 100 cm length aluminum core. A 220 cm long aluminum annulus of 7.62 cm thickness surrounded this graphite & aluminum core. The worst case situation is for the \bar{p} production target out, with maximum heating occurring just after the beam enters a material (C, Al, Fe). The results are insensitive to the details of the dump geometry at large radial distances, since the cascade on the average propagates outward from the beam region. The beam spot was assumed to have a Gaussian profile with $\sigma_x = \sigma_y = 0.04$ cm. Bin sizes were $\Delta Z = 22$ cm and $\Delta r = 0.04$ cm. Fig. 8 shows the resulting enthalpy increase due to the beam energy deposition versus the distance from the target, for the innermost radial bin. Based on the maximum enthalpy reserve as a function of temperature calculated for each material (Fig. 9), a temperature increase was obtained for a pulse of 3×10^{12} protons, as shown in Table I. A local temperature increase of $\sim 115^\circ\text{C}$ is predicted in the graphite (on the beam axis). The aluminum and iron sections (on axis) increase in temperature by no more than $\sim 15^\circ\text{C}$. Thus, conditions are far from the melting points of any of these materials.

III. Total Energy Deposited in the Dump

The total energy deposited in the graphite and aluminum parts of the dump shown in Fig. 7, is ~ 60 GeV/proton. This corresponds to an average power dissipation of 14.4 kW for a 2 second cycle and 3×10^{12} incident protons. It is interesting to compare these numbers with the Tevatron abort dump in which the maximum temperature increase in the graphite core was calculated to be $\Delta T=880^\circ\text{C}$ and the average power input to the cooling loops was 139 kW for a 23 sec cycle time and 2×10^{13} protons per pulse. Based on the results in this note, the cooling requirements and melting considerations are much less severe for the \bar{p} proton beam dump. Even though the beam spot is much smaller in this case, the dump heating is reduced significantly due to the lower energy and beam intensity.

The energy deposited in the iron shielding surrounding the dump core is 69 GeV/proton. Thus, a total of 129 GeV/proton is deposited in the entire dump (C + Al + Fe). The shielding has an outer, radial limit of $r=137$ cm and longitudinal limits of $213.2 \text{ cm} < Z < 1100 \text{ cm}$, resulting in an overall dump length of 887 cm. This is comparable to the Tevatron abort dump length of 850 cm. The dump core is recessed into the shielding by 176.8 cm. With the 220 cm core length, this results in 490 cm of iron after the downstream end of the core, compared to ~ 405 cm from the Tevatron abort dump.

The actual radial dimensions of the steel shielding surrounding the dump core will be somewhat larger than the limits used in the present calculations. The limit of $r=137$ cm represents the minimum transverse dimension that is in the dump shielding design. The longitudinal limits used are quite close to the values in the design. Thus, the actual energy deposition in the iron shielding should be quite similar to that calculated here.

IV. Conclusions

- (1) From an energy deposition viewpoint, a beam dump consisting of a 7.62 cm radius graphite core of 120 cm length, followed by a 7.62 cm radius aluminum core of 100 cm length, and surrounded by an aluminum annulus of 7.62 cm thickness, is adequate.
- (2) The addition of a 7.62 cm aluminum annulus around the core of the dump results in a more uniform distribution of energy deposition throughout the dump.
- (3) Local melting of the dump core along the beam axis will not occur, due to the relatively low peak energy deposition per pulse.
- (4) 40% of the total beam energy of 150 GeV is deposited within the graphite and aluminum parts of the dump. 86% of the total energy is deposited in the entire dump, including the iron shielding.

- (5) The cooling system should dissipate a minimum of 14 kw from the C-A2 core and annulus.

References

- (1) CASIM, A. Van Ginnekin, Fermilab FN-292 (1975).
- (2) Tevatron I Design Report, Fermilab, 1983.
- (3) IEEE Transactions on Nuclear Science, Vol. NS-28 No. 3, June 1981,
pg. 2774.

Table I

Peak Energy Density (ϵ) and Temperature Increase (ΔT) for the TeV I \bar{p}
 Target Hall Proton Beam Dump ($N_p = 3 \times 10^{12}$)

Material	ρ (gm/cm ³)	Peak ϵ (GeV) (cm ³ -proton)	Peak H (J/gm)	Peak ΔT (°C)
C	1.8	0.33	88	~ 115
Al	2.7	0.083	14.8	~ 15
Fe	7.9	0.017	1.03	~ 15

Figure Captions

- Fig. 1. (a) Energy deposition per incident proton per bin ($\Delta r=7.62$ cm, $\Delta Z=22$ cm) versus longitudinal distance from target position. \bar{p} production target in. 170 cm graphite core.
(b) Target out.
- Fig. 2. (a) Energy deposition per incident proton per bin ($\Delta r=7.62$ cm, $\Delta Z=22$ cm) versus longitudinal distance from target position. Target in. 120 cm graphite + 50 cm aluminum core.
(b) Target out.
- Fig. 3. (a) Energy deposition per incident proton per bin ($\Delta r=7.62$ cm, $\Delta Z=22$ cm) versus longitudinal distance from target position. Target in. 120 cm graphite + 100 cm aluminum core.
(b) Target out.
- Fig. 4. (a) Energy deposition per incident proton per bin ($\Delta r=7.62$ cm, $\Delta Z=22$ cm) versus longitudinal distance from target position. Target in. 120 cm graphite + 100 cm aluminum core, + 7.62 cm aluminum annulus.
(b) Target out.

Fig. 5. (a) Energy deposition per incident proton per bin ($\Delta r=7.62$ cm, $\Delta Z=22$ cm) versus longitudinal distance from target position. Target in. 120 cm graphite + 75 cm aluminum core + 7.62 cm aluminum annulus.

(b) Target out.

Fig. 6. (a) Energy density per proton per bin ($\Delta r=7.62$ cm, $\Delta Z=22$ cm) versus longitudinal distance from target position. Target in. 120 cm graphite + 100 cm aluminum + 7.62 cm aluminum annulus.

(b) Target out.

Fig. 7. Schematic, cut-away drawing of the \bar{p} target hall proton beam dump "optimum" geometry.

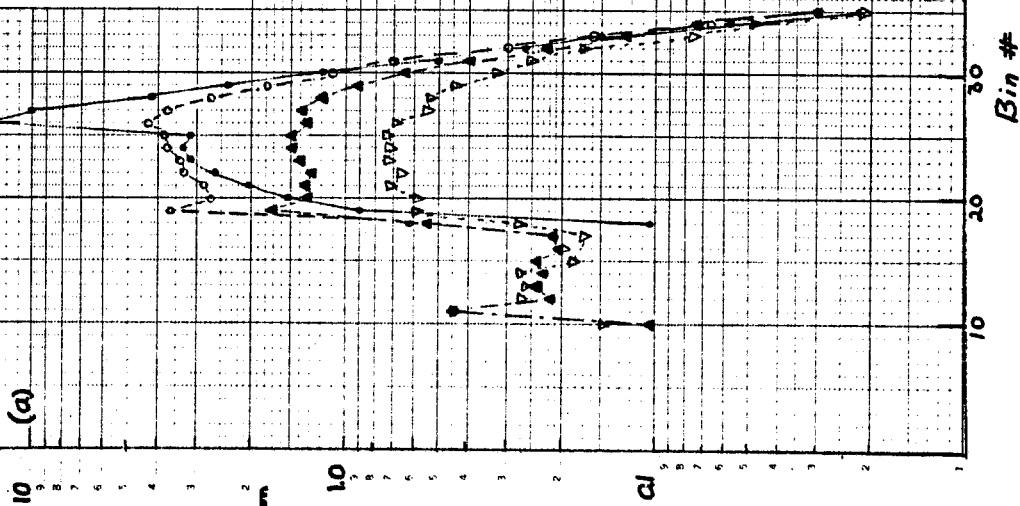
Fig. 8. (a) Enthalpy increase versus longitudinal distance for the dump in Fig. 7. Target out. Used to estimate maximum temperature rise in dump materials.

Fig. 9. Enthalpy reserve vs maximum temperature for several materials.

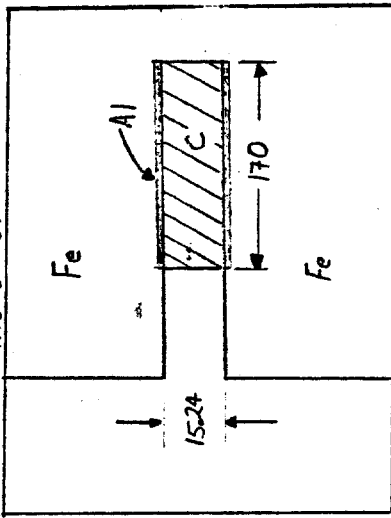
Energy Deposition

W	Fe	C	Al	Total
2.01	103.8	18.1	3.5	127.5

(a)



Not to Scale



Energy Deposition

W	Fe	C	Al	Total
0.0	106.4	20.8	2.6	129.8

(b)

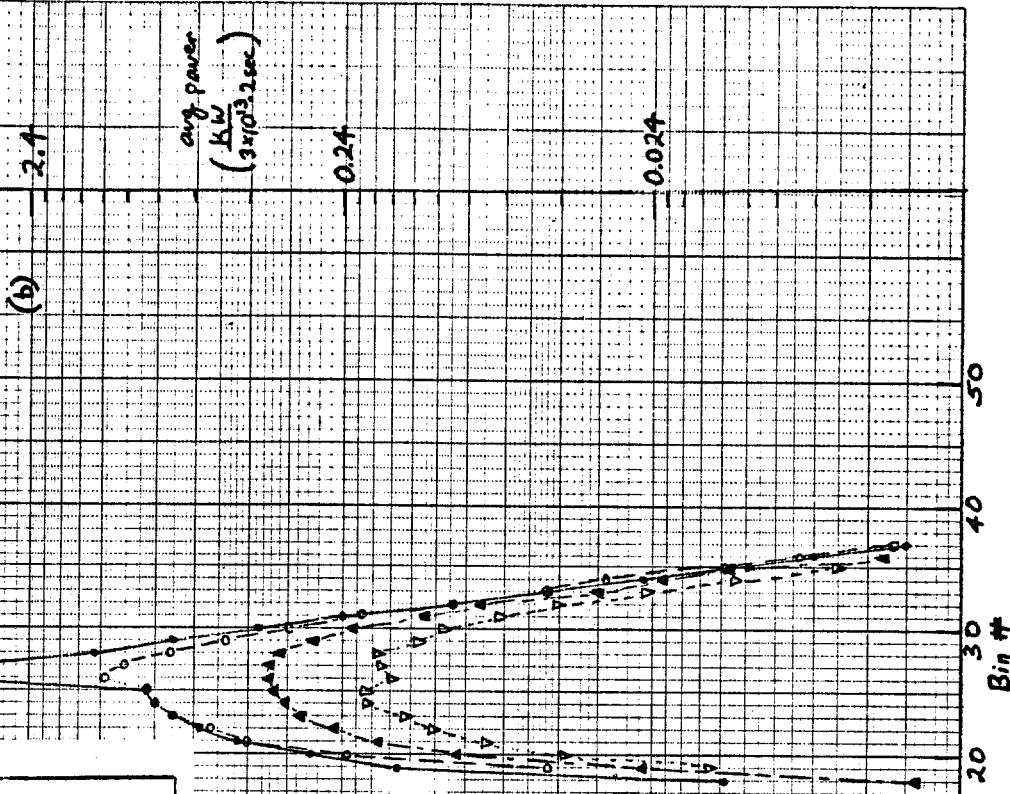


Fig 1.

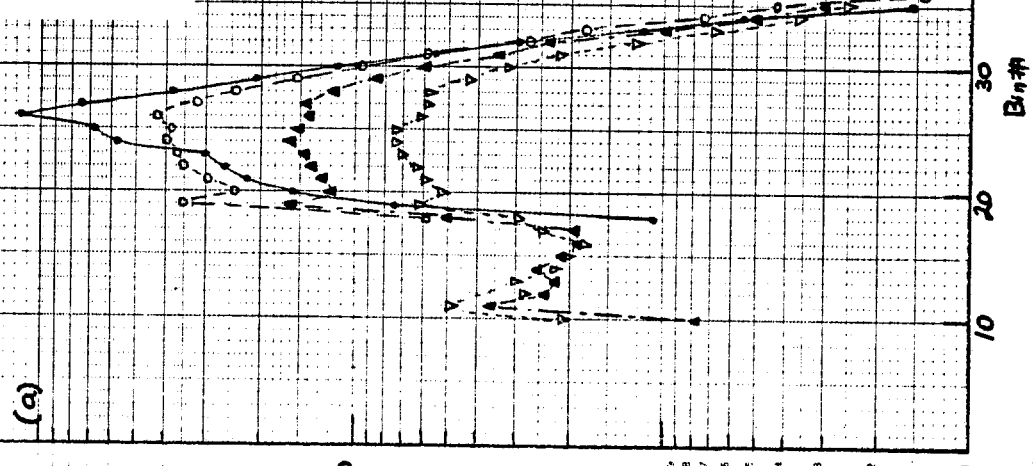
Bin #

Bin #

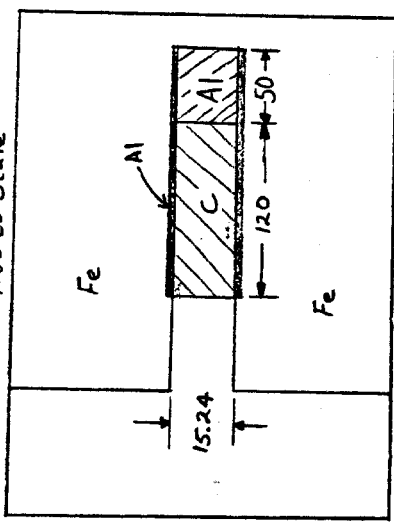
Energy Deposition (GeV)

W	Fe	C	Al	Total
2.09	9.0	11.0	18.1	40.2

(a)



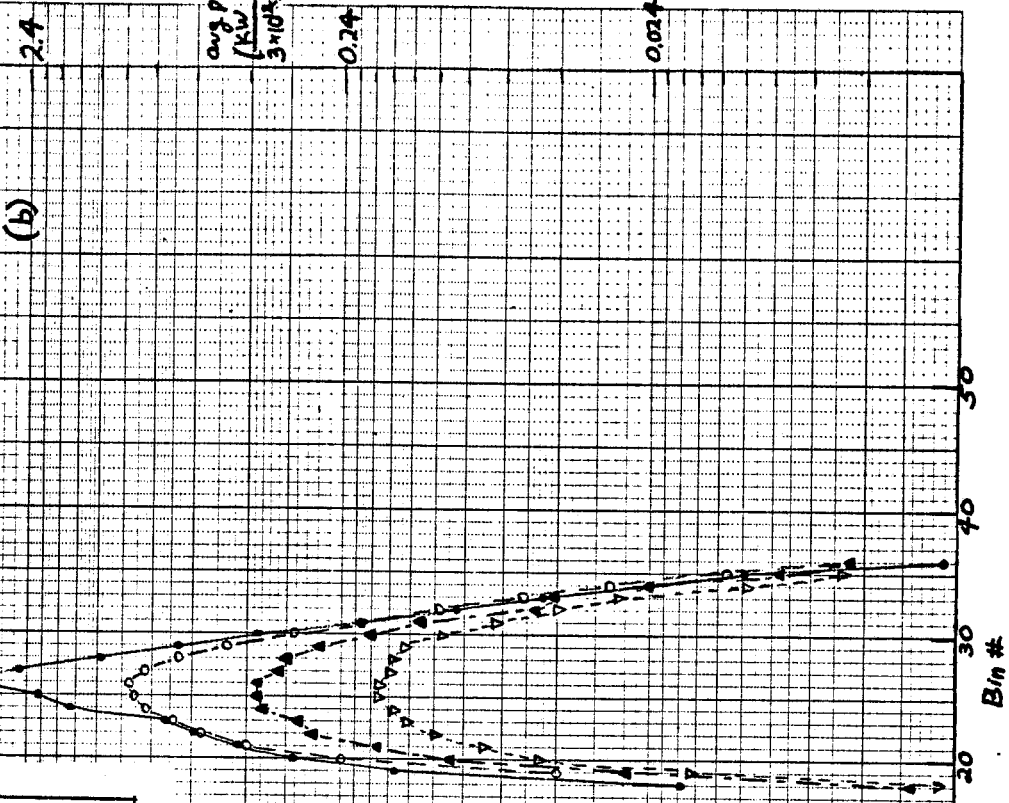
Not to Scale



Energy Deposition

W	Fe	C	Al	Total
0.0	95.0	11.7	22.5	129.2

(b)



avg power
 (kW)
 $\frac{3 \times 10^{12} \times 2000}{3}$

0.74

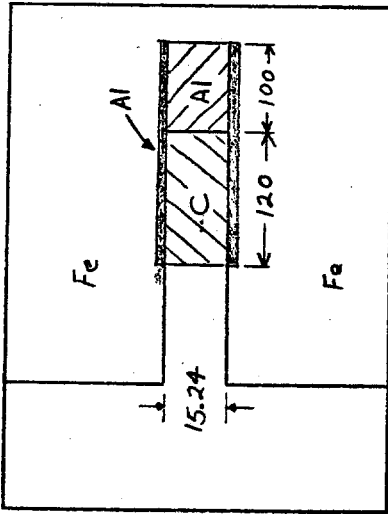
0.024

Bin #

Fig 2

Bin #

Not to Scale



Energy Deposition

W	Fe	C	Al	Total
2.1	109	238	127.3	

(a)

10

46 6010

GeV
inc proton

1.0

KM SEMI-LOGARITHMIC CYCLES X 20 DIVISIONS
REVISED 8/19/60 W.M.H.

10
9
8
7
6
5
4
3
2
1

Bin #

10

20

30

40

50

Fig. 3

10

20

30

40

50

Energy Deposition

W	Fe	C	Al	Total
0.0	81.6	17.5	36.4	127.3

(b)

2.1

Avg Power
(KW/3x10¹² 2sec)

0.24

0.024

Bin #

10

20

30

40

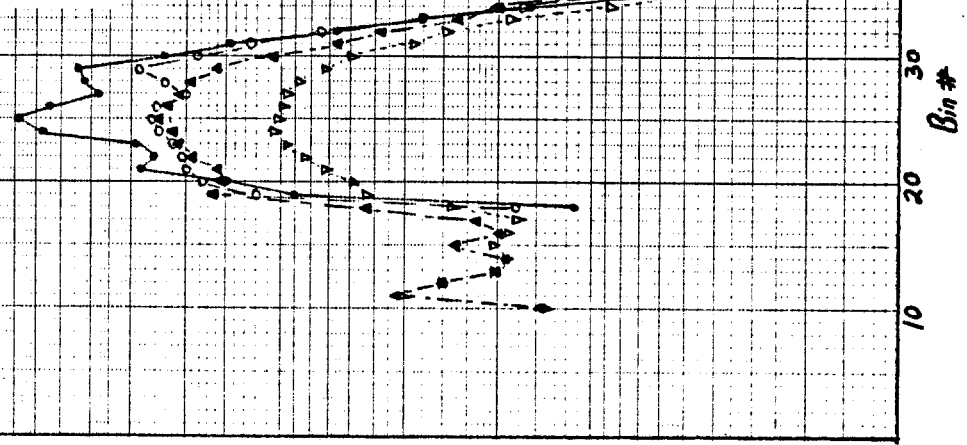
50

GeV
100 proton

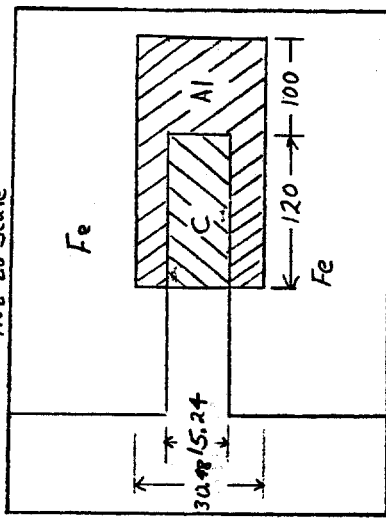
Energy Deposition

W	Fe	C	Al	Total
205	71.4	10.7	13.2	127.4

(a)



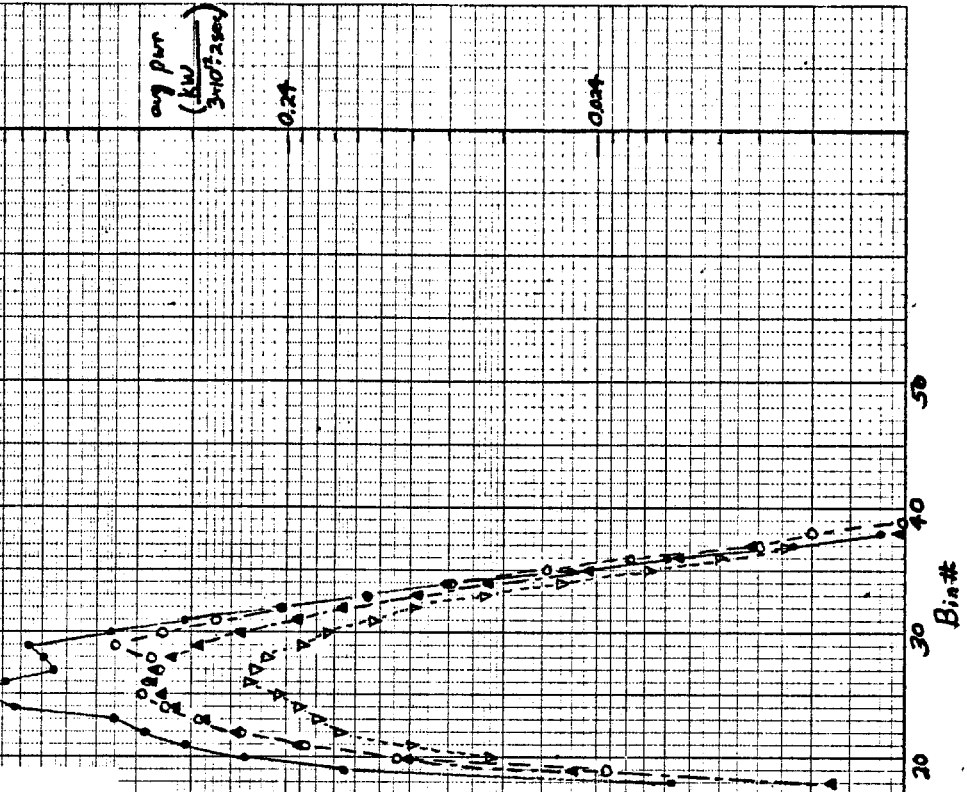
Not to Scale



Energy Deposition

W	Fe	C	Al	Total
0.0	58.9	11.2	48.8	128.8

(b)

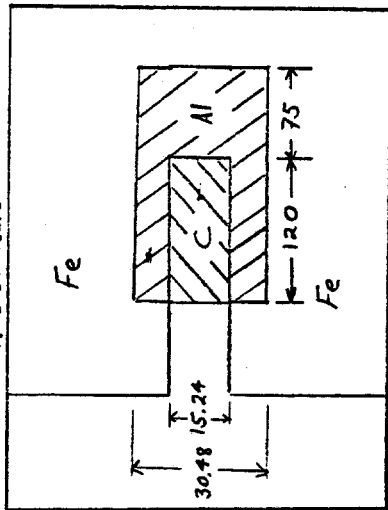


Bin #

Bin #

Bin #

Not to Scale



Energy Deposition

W	Fe	C	Al	Total
228	76.7	10.9	37.8	1237

(a)

46 6010

GeV
10¹¹ proton

K-M SEMI LOGARITHMIC CYCLES & DIVISIONS
RUPPEL & BROWN CO. MINNEAPOLIS

Energy Deposition

W	Fe	C	Al	Total
90	76.3	11.3	91.8	178.4

(b)

avg pow
(KW
3·10¹²·150e)

0.24

0.034

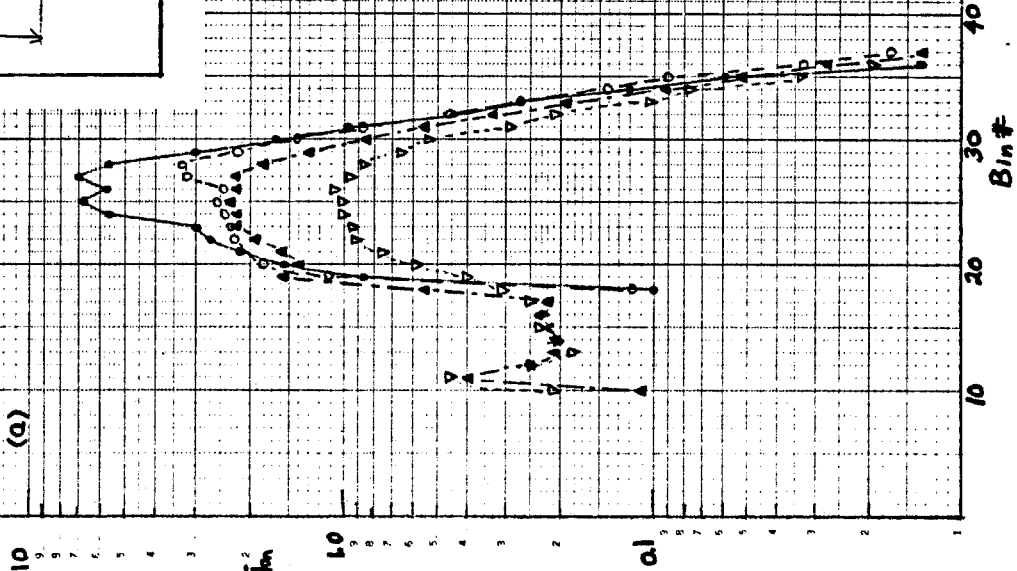
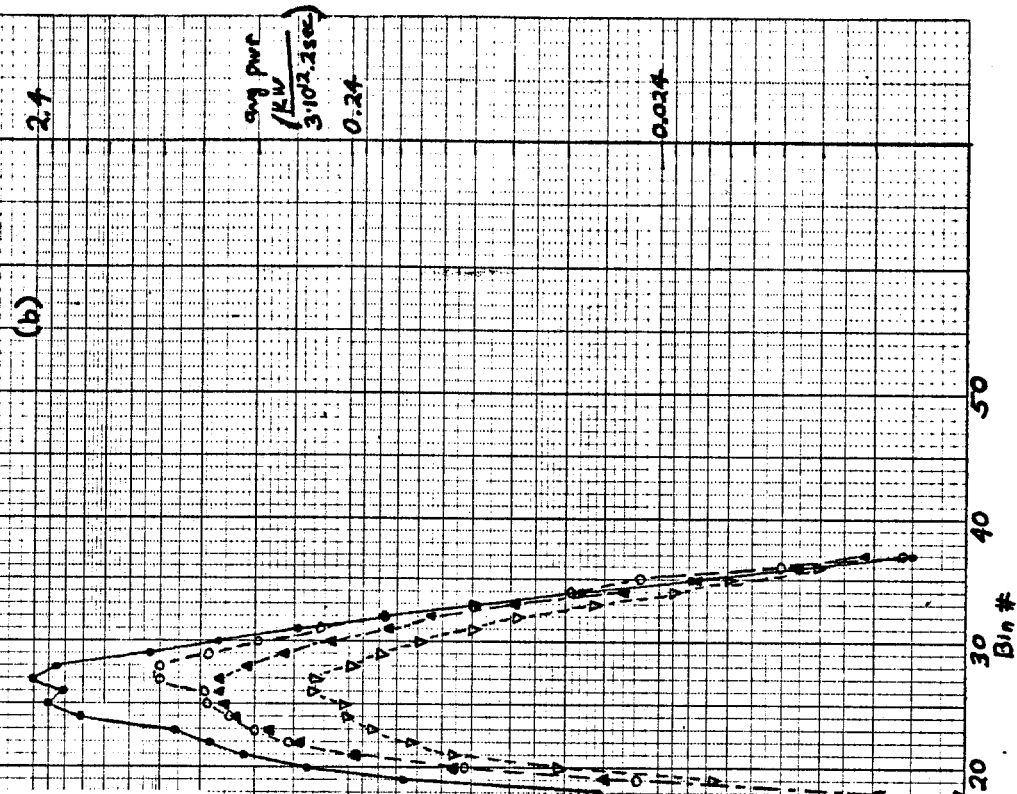


Fig 5

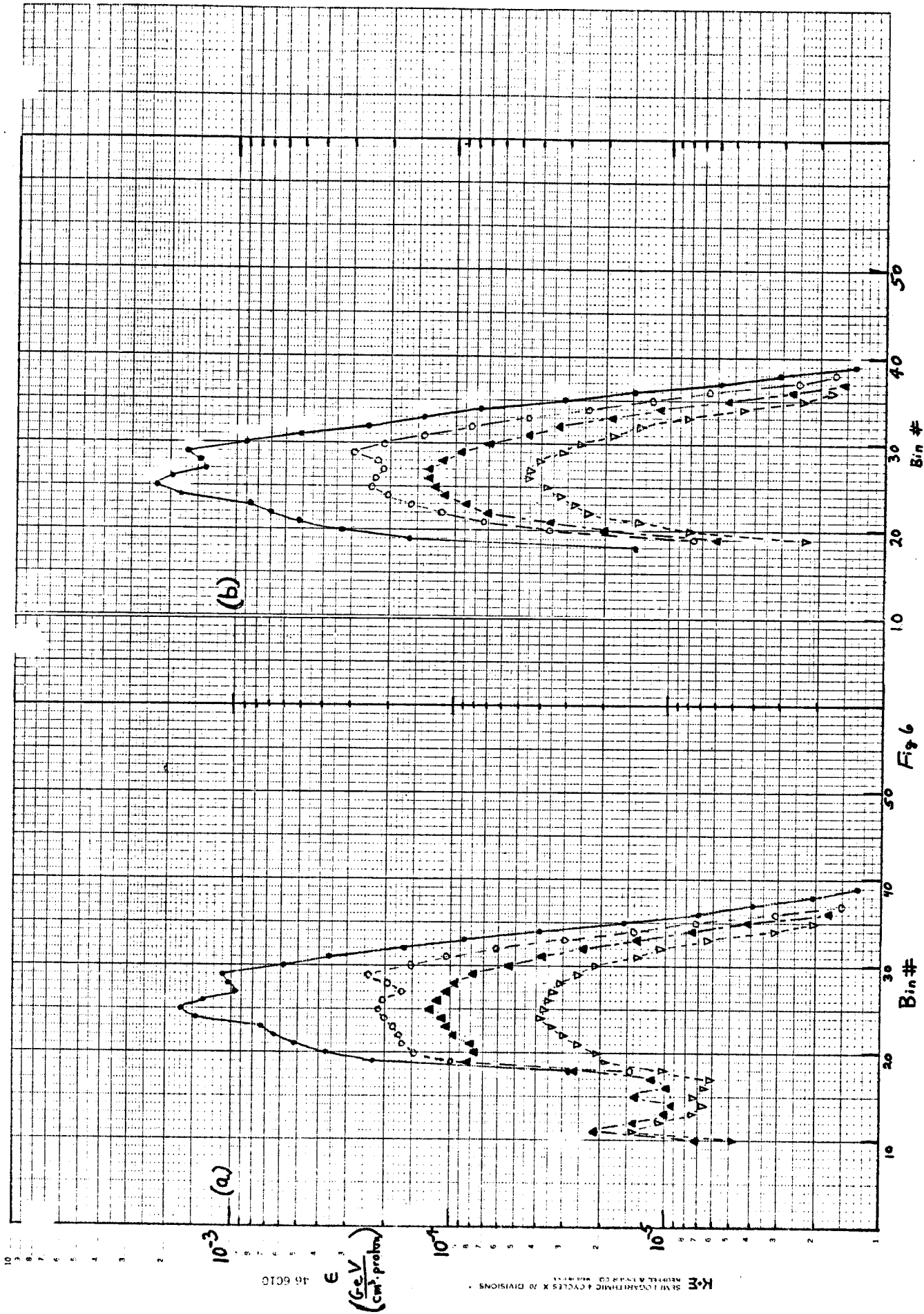
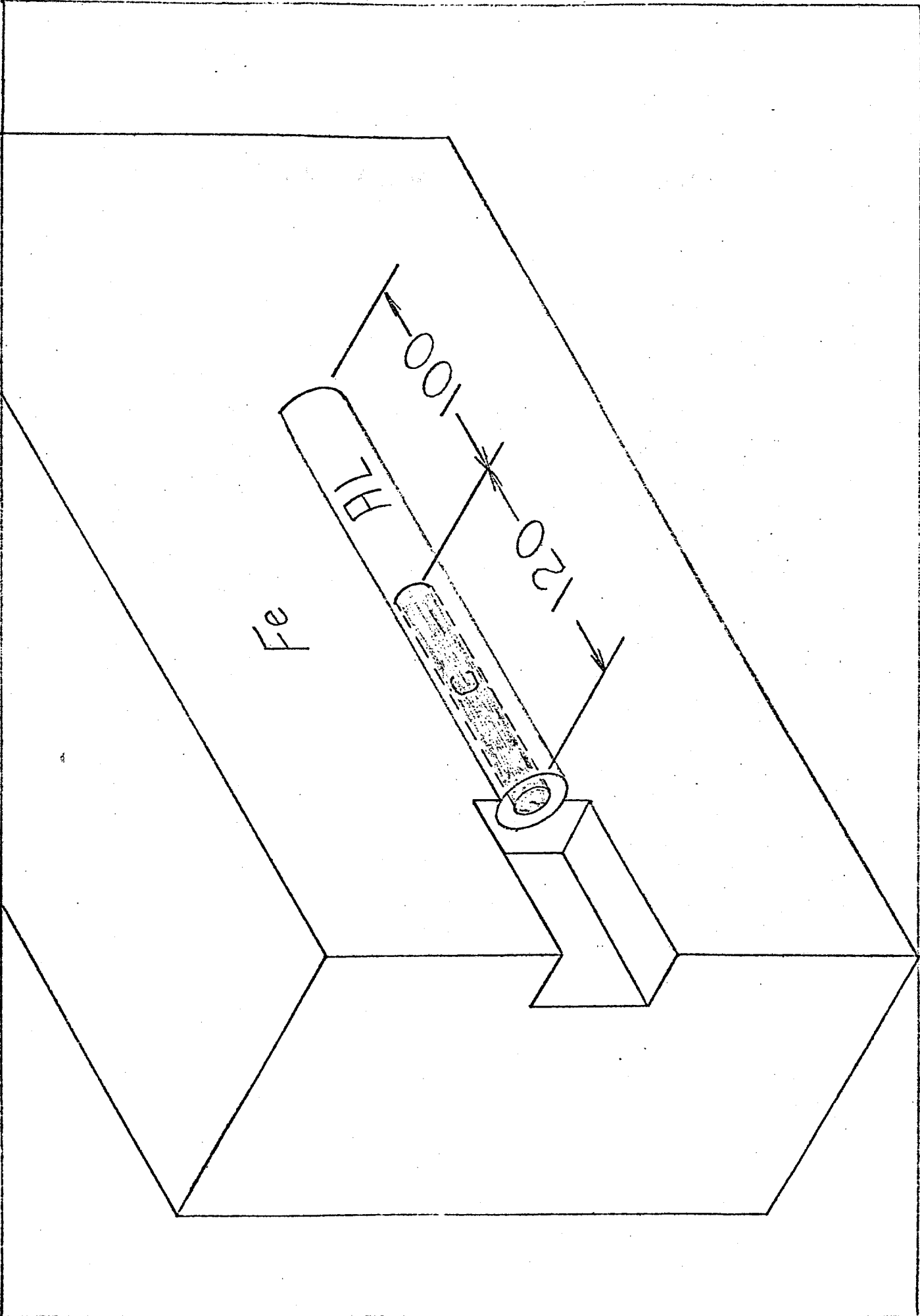
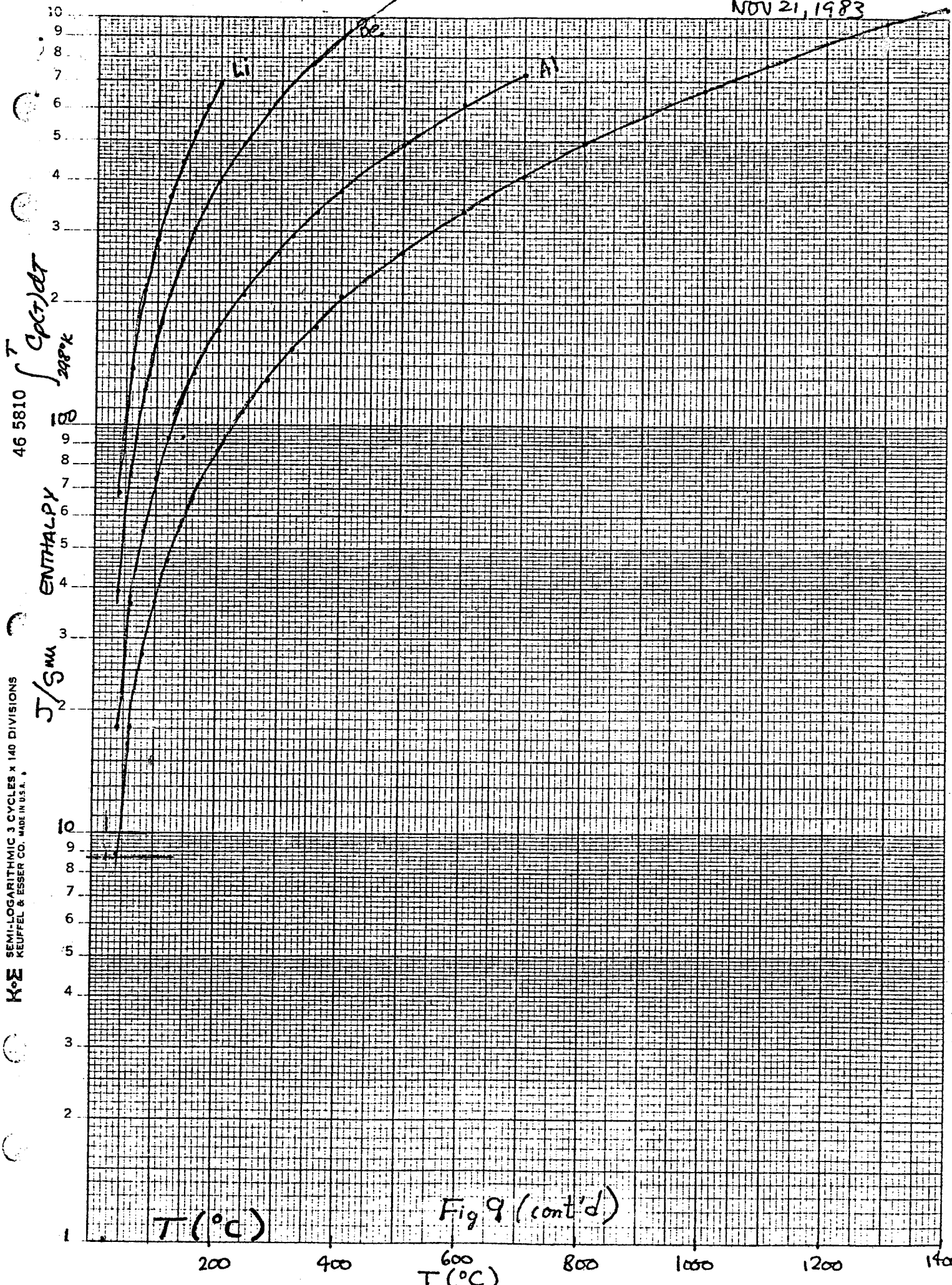


Fig 6



NOV 21, 1983



46 5810 $\int_{298^{\circ}K}^T C_p(T) dT$

ENTHALPY

J/sma

K&E SEMI-LOGARITHMIC 3 CYCLES x 140 DIVISIONS KEUFFEL & ESSER CO. MADE IN U.S.A.

T(°C)

Fig 9 (cont'd)

T(°C)